Identification of RR Lyrae Stars in the Milky Way Nuclear Star Cluster

Hui Dong[1], Rainer Schödel[1], Benjamin Williams[2], Tuan Do[3], Andrea Ghez[3], Mark Morris[3], Michael Rich[3], Francisco Nogueras-Lara[1], Eulalia Gallego-Cano[1], Teresa Gallego-Calvente[1], Daniel Wang[4] and Zhiyuan Li[5]

1. Instituto de Astrofísica de Andalucía (CSIC), Glorieta de la Astronomía S/N, E-18008 Granada, Spain
2. Department of Astronomy, Box 351580, University of Washington, Seattle, WA 98195, USA
3. Department of Physics and Astronomy, University of California, Los Angeles, CA, 90095, USA
4. Department of Astronomy, University of Massachusetts, Amherst, MA, 01003, USA
5. School of Astronomy and Space Science, Nanjing University, Nanjing, 210093, China

We present our recent efforts to use RR Lyrae type ab (RRab) stars to constrain old metal-poor stellar populations in the Milky Way nuclear star cluster. From the four-year baseline *HST*/WFC3/IR observations of the central $2.3' \times 2.3'$ of the Milky Way, we found four RRab and three candidates. Specifically, they fall exactly onto the Oosterhoff I division in the Bailey diagram. The extinction and distance of one RRab match those of the nuclear star cluster given in previous works. We performed simulations and found that after correcting for incompleteness, there could be no more than 40 RRab stars within the nuclear star cluster and in our field-of-view. Through comparing with the known globular clusters of the Milky Way, we estimated that if there exists an old metal-poor ($-1.5 < [\mathrm{Fe/H}] < -1$) stellar population in the Milky Way nuclear star cluster, then it contributes at most $\sim 18\%$ of the total stellar mass of the nuclear star cluster.

1 Motivation

The Milky Way's Nuclear Star Cluster (MWNSC hereafter) is the closest NSC ($\sim$8 kpc from us, Boehle et al., 2016). It is the best lab for us to study the origin of NSC: *in-situ* star formation (Agarwal & Milosavljević, 2011) and/or infall globular clusters (Antonini et al., 2012). In the former scenario, the NSC consists of stellar populations with wide ranges of ages and metallicities, while the latter scenario only predicts old metal-poor stellar populations.

The MWNSC has a half-light radius of approximately 4 pc and a total mass of roughly $2.5 \times 10^7\,\mathrm{M}_\odot$. The cluster's rotation axis is parallel to that of the Galactic disk. The cluster is also known to have a quasi-continuous, complex star formation history (Pfuhl et al., 2011). The most recent burst of star formation in the MWNSC happened $\sim 3 - 6$ Myr ago (e.g., Lu et al., 2013).

While the most recently formed stars are generally believed to have formed *in situ* (Lu et al., 2013), there is still no compelling evidence for the presence of a

stellar population that may have been contributed by infall globular clusters. As a first step, finding such evidence requires identifying $\sim 10\,\mathrm{Gyr}$ old stars and deriving their metallicities. However, because of the extreme interstellar extinction and strong source crowding toward the Galactic center (GC), current spectroscopic studies with adaptive optics (AO) assisted 8m-class telescopes are generally limited to $K_s \leq 16\,\mathrm{mag}$ (Pfuhl et al., 2011). The mean mass of the spectroscopically accessible, $K_s = 15 - 16\,\mathrm{mag}$ Red Clump (RC) giants is $> 1\,\mathrm{M}_\odot$ (see fig. 16 in Schödel et al., 2007), which means that they may not be old enough to serve as potential tracers of ancient globular cluster infall.

RR Lyrae (RRL) stars provide us with a method to study the old metal-poor stellar populations ($> 10\,\mathrm{Gyr}$ old). RRL stars are low-mass core-helium-burning stars with oscillation amplitudes in the $0.1 < \delta K_s < 0.5$ mag range and period range between about 0.2 and 1 d. The majority of RRLs are found in metal-poor globular clusters (Catelan, 2009). Based on the period-amplitude diagram of such RRLs (also known as a Bailey diagram), the globular clusters in the Milky Way can be divided into two types: Oosterhoff type I and II (OoI and OoII, hereafter). In general, the OoI clusters ([Fe/H] $\sim [-1.0, -1.5]$) seem to be more metal-rich than the OoII clusters ([Fe/H] $\sim [-1.5, -2.5]$) (fig. 5 in Catelan 2009). Therefore, by 0finding RRL stars and determining their distribution between these two types, we can provide new constraints on the formation history of the MWNSC.

The biggest challenge to detecting RRL stars in the MWNSC is their intrinsic faintness. Accounting for the appropriate extinction and distance modulus of the GC, their observed magnitudes are $K \approx 17\,\mathrm{mag}$ and $H \approx 18.5\,\mathrm{mag}$, below the detection threshold of the seeing-limited (FWHM $\approx 0.7''$) VISTA Variables in the Via Lactea Survey (VVV) that consists of multi-epoch near-infrared (near-IR) imaging observations of the Galactic bulge and southern disk since 2010 (Minniti et al., 2010). Although Minniti et al. (2016) recently reported the detection of RRL stars in the Galactic Nuclear bulge, the locations and relatively low extinctions of these stars suggest that they are in the foreground of the Galactic bulge.

2 *HST*/WFC3 Observations

We used the four-year baseline *HST*/WFC3 observations (2010–2014) of the MWNSC at the F153M band ($1.53\,\mu$m) to detect RRL stars. Especially, several observation blocks in 2014 are long: 10 hours on Feb 28, 10 hours on Mar 10, 15 hours on April 2, and 5.5 hours on April 3. These blocks are critical in our identification of RRL stars, because of the significant coverage of their periods. We also employed the single-epoch *HST*/WFC3 observations at the F127M band ($1.27\,\mu$m) to determine F127M–F153M colours, which help to locate individual stars in the foreground/background or in the MWNSC proper.

We used 'DOLPHOT' to detect sources, to extract photometry from individual dithered exposures, and empirically to determine the photometric variations among exposures (Dong et al., 2017a). We further used the least χ^2 method to identify variable stars, and then the Lomb-Scargle periodogram analysis to calculate the periods of 36 sources with well-covered light curves within the individual observation blocks in 2014. We found that 21 sources have periods between 0.2 and 1 d, and therefore could be RRL stars. Fig. 1 shows a mosaic image from the *HST*/WFC3 F153M observations overlaid with the positions of the 21 sources. Fig. 2 gives the

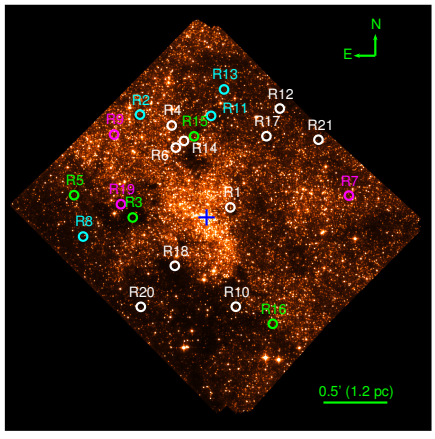

Fig. 1: *HST* WFC3/IR F153M observations of the MWNSC. The blue plus marks the central massive black hole, Sgr A*. The green circles are the four variables with typical RRab light curves. The cyan circles mark RRc candidates, magenta ones RRab candidates, and white ones eclipsing binary candidates.

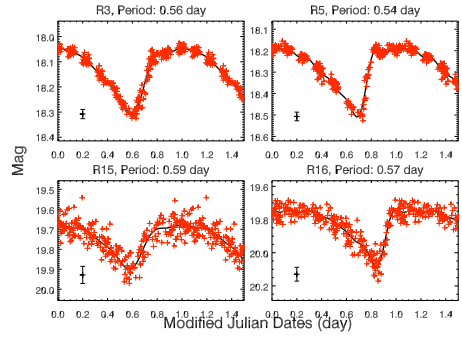

Fig. 2: The folded F153M light curves for four RRab stars. In the title of each figure, we give the source IDs and periods. The black pluses in the left bottom corner of the individual panels show the average photometric variation among dithered exposures derived from the artificial star tests, plus 0.01 mag systematic uncertainty. The black solid lines are from the DFF fitting.

folded light curves of four of the 21 sources.

Besides the periods, from the *HST*/WFC3 observations, we also derived the following parameters for these candidates:

- Amplitudes. We used the direct Fourier fitting (DFF) method (Kovács & Kupi, 2007) to analyze the folded light curves of these 21 variable stars. Then, we can obtain the mean F153M magnitudes and the peak-to-peak amplitudes;
- Extinctions and distances. We first derived the mean F127M magnitude from the observed F127M magnitude and the DFF fitting of the folded F153M light curves, but with different amplitude (Dong et al., 2017b). Then, we derived the extinctions and distances for individual candidates, assuming the period-luminosity relationship of the RRL stars (Catelan et al., 2004) and the extinction curve of (Schödel et al., 2010).

3 Classification

Of the 21 candidates, only four show the typical sawtooth light curves and are definitely RRab stars (Fig. 2). The other candidates with sine-shaped light curves could also be W UMa stars, which are eclipsing low-mass overcontact binaries and have periods between 0.2 to 1 d too. W UMa stars are intrinsically fainter than RRL stars.

We compared the extinction and distance of the 21 stars with the ones of the MWNSC, which are well-determined in previous references (e.g. Boehle et al., 2016; Schödel et al., 2010). If the candidates are W UMa stars, in Sect. 2 we would

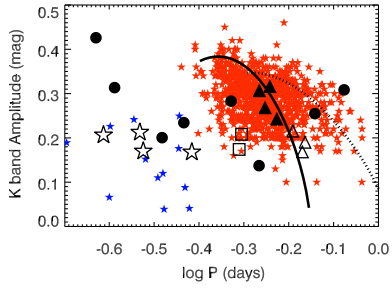

Fig. 3: Bailey diagram: K-band amplitude plotted against the logarithm of the period of RRL stars. The small red and blue stars represent the RRab and RRc stars detected in the Galactic bulge by the VVV survey (Gran et al., 2015, 2016). The large symbols are our variable stars with periods between 0.2 and 1 d: Open stars for RRc candidates, filled triangles for identified RRab stars, open triangles for RRab candidates, filled circles for identified eclipsing binary candidates, and two open boxes for stars that may be RRab or eclipsing binaries. The black solid and dashed lines are the OoI and Oo II lines from Navarrete et al. (2015).

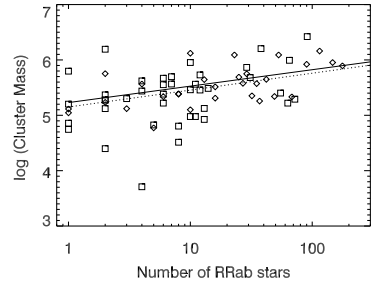

Fig. 4: The relationship between the number of RRab stars and the logarithm of cluster mass in units of solar mass for the OoI (diamonds) and OoII (squares) clusters. The solid (OoI) and dashed (OoII) lines represents the Eqns. 11 and 12 in Dong et al. (2017b), respectively.

overestimate their distances with the period-luminosity relation of RRL stars. We found that all the 21 stars have extinction less than that of the MWNSC, but eight of them are far away from the MWNSC by three times the corresponding uncertainties. Because stars behind the MWNSC should also have to suffer extra extinction, the lower extinction and large distance of these eight sources are unphysical. Therefore, we classified them as eclipsing binaries.

Fig. 3 shows the Bailey diagram for our sources along with the data for a reference sample of RRab (Gran et al., 2016) and RRc stars (Gran et al., 2015) derived from the VVV survey. The eight eclipsing binaries defined above are widely distributed throughout the Bailey diagram. We classified another two sources (open boxes) as eclipsing candidates because they do not fall on the Oosterhoff lines given in Fig. 3. The other candidates lie perfectly within the range for the RRL stars from the VVV survey. To summarise, our 21 sources include four RRc stars, four RRab stars, three RRab candidates, as well as ten probable eclipsing binaries.

4 Old Metal-Poor Stellar Populations in the MWNSC

Through comparing the extinctions and distances of the four RRab stars with sawtooth light curves to those of the MWNSC, we suggest that one RRab is in the MWNSC, while two are in front and one behind the MWNSC. Because all these

four RRab stars fall in the OoI line in the Bailey diagram, the metallicity ([Fe/H]) of the corresponding old metal-poor population should be between -1.5 and -1.

We used the detected RR Lyrae stars to constrain the mass and metallicity of the old, metal-poor stellar populations in the MWNSC. First, we performed the simulation to correct the detection limit in the central few tens of arcsecond. We found that there could be ten RRab stars, but at most 40 RRab stars can be in the MWNSC. Second, we used the MW globular clusters to derive the relationship between the number of RRab stars in each cluster and the total mass, which is given in Fig. 4. Third, with this relationship, we translate the number of RRab stars into the total mass of old metal-poor stellar populations in the MNWSC. We found that the OoI globular clusters with $-1.5 < [\mathrm{Fe/H}] < -1$ contributes at most 18% of the total stellar mass in the MNWSC, and the OoII globular clusters with $-2.5 < [\mathrm{Fe/H}] < -1.5$ contributes at most 13%. Therefore, it means that the infall of globular clusters play a small role in the construction of the MWNSC, which is consistent with the results given in Do et al. (2015) and Feldmeier-Krause et al. (2017).

Acknowledgements. We thank the organizer, Radek Smolec, to give us this chance to present our work in this RR Lyrae workshop.

References

Agarwal, M., Milosavljević, M., *ApJ* **729**, 35 (2011), arXiv: 1008.2986

Antonini, F., Capuzzo-Dolcetta, R., Mastrobuono-Battisti, A., Merritt, D., *ApJ* **750**, 111 (2012), arXiv: 1110.5937

Boehle, A., et al., *ApJ* **830**, 17 (2016), arXiv: 1607.05726

Catelan, M., *Ap&SS* **320**, 261 (2009), arXiv: astro-ph/0507464

Catelan, M., Pritzl, B. J., Smith, H. A., *ApJS* **154**, 633 (2004), arXiv: astro-ph/0406067

Do, T., et al., *ApJ* **809**, 143 (2015), arXiv: 1506.07891

Dong, H., et al., *MNRAS* **470**, 3427 (2017a), arXiv: 1706.03243

Dong, H., et al., *MNRAS* **471**, 3617 (2017b), arXiv: 1706.03299

Feldmeier-Krause, A., et al., *MNRAS* **464**, 194 (2017), arXiv: 1610.01623

Gran, F., et al., *A&A* **575**, A114 (2015), arXiv: 1501.00947

Gran, F., et al., *A&A* **591**, A145 (2016), arXiv: 1604.01336

Kovács, G., Kupi, G., *A&A* **462**, 1007 (2007), arXiv: astro-ph/0610823

Lu, J. R., et al., *ApJ* **764**, 155 (2013), arXiv: 1301.0540

Minniti, D., et al., *New A* **15**, 433 (2010), arXiv: 0912.1056

Minniti, D., et al., *ApJ* **830**, L14 (2016), arXiv: 1610.04689

Navarrete, C., et al., *A&A* **577**, A99 (2015), arXiv: 1501.02286

Pfuhl, O., et al., *ApJ* **741**, 108 (2011), arXiv: 1110.1633

Schödel, R., Najarro, F., Muzic, K., Eckart, A., *A&A* **511**, A18 (2010)

Schödel, R., et al., *A&A* **469**, 125 (2007), arXiv: astro-ph/0703178